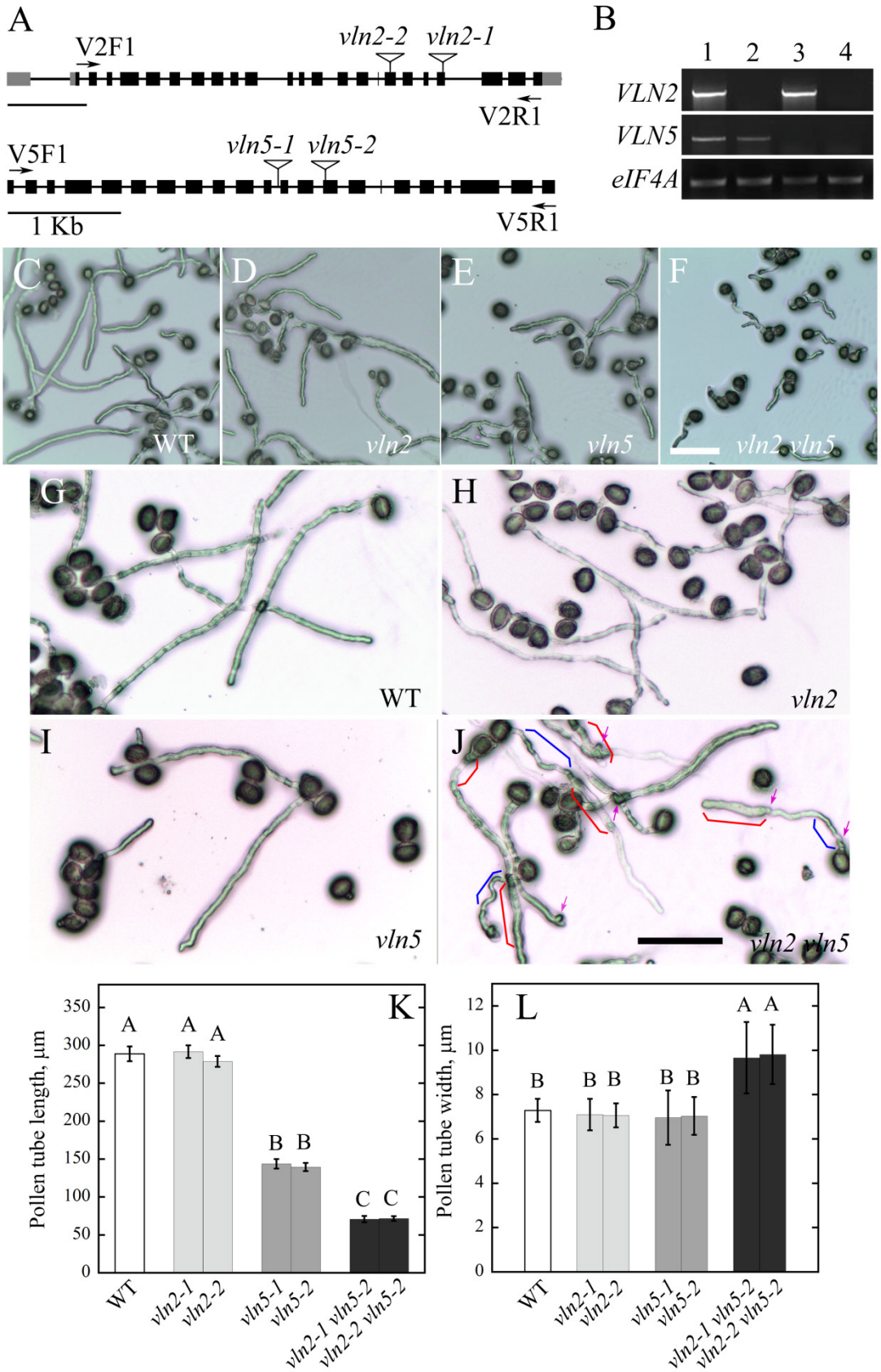
A
V2F1
vln2-2
vln2-1
V2R1
V5F1
vln5-1
vln5-2
1 Kb
V5R1
B
1
2
3
4
VLN2
VLN5
eIF4A
C
WT
D
vln2
E
vln5
F
vln2 vln5
G
WT
H
vln2
I
vln5
J
vln2 vln5
K
Pollen tube length, μm
350
300
250
200
150
100
50
0
A
A
A
B
B
C
C
WT
vln2-1 vln2-2
vln5-1 vln5-2
vln2-1 vln5-2 vln2-2 vln5-2
L
Pollen tube width, μm
12
10
8
6
4
2
0
B
B
B
B
B
A
A
WT
vln2-1 vln2-2
vln5-1 vln5-2
vln2-1 vln5-2 vln2-2 vln5-2

Supplemental Figure 1. *VLN2* and *VLN5* Coordinately Regulate Polarized Pollen Tube Growth

(A) Schematic showing the structures of *VLN2* and *VLN5*. Untranslated regions, exons, and introns are represented by gray boxes, black boxes, and black lines, respectively. Insertion sites indicated for the T-DNA insertion lines *vln2-1* and *vln2-2*, *vln5-1* and *vln5-2* were reported in Bao *et al*. (2012) and Zhang *et al*. (2010a), respectively.

(B) RT-PCR analysis for *vln2 vln5* double mutant revealed that both *VLN2* and *VLN5* full-length transcripts were absent in *vln2-2 vln5-2*. *vln2-2*, *vln5-2* and *vln2-2 vln5-2* were selected for RT-PCR analysis. The experiment was repeated three times. The result showed that *VLN2* and *VLN5* full-length transcripts were absent in *vln2-2* and *vln5-2*, respectively, consistent with previous studies (Zhang et al., 2010a; Bao et al., 2012). Both *VLN2* and *VLN5* full-length transcripts were absent in *vln2-2 vln5-2*. *eIF4A* was selected as the internal loading control. Lane 1, wide-type Col-0 (WT); Lane 2, *vln2-2*; Lane 3, *vln5-2*; Lane 4, *vln2-2 vln5-2*.

(**C-F**) Micrographs of pollen tubes after incubation for 2.5 h in germination medium. (**C**) WT, (**D**) *vln2-2*, (**E**) *vln5-2*, and (**F**) *vln2 vln5*. Scale bar = 100 μm.

(**G-J**) Micrographs of pollen tubes after the average tube lengths reached about 300 μm. The micrographs were captured under high magnification in order to clearly visualize the morphology of pollen tubes. (**G**) WT, (**H**) *vln2-2*, (**I**) *vln5-2*, and (**J**) *vln2 vln5*. The morphology of *vln2 vln5* pollen tubes is abnormal; red lines and blue lines indicate the wide and narrow regions along pollen tubes, respectively. Pink arrows indicate curvatures on pollen tubes. Scale bar = 100 μm.

(**K**) Pollen tube length was significantly decreased in *vln2 vln5* plants. Plants of different genotypes were incubated for 2 h in germination medium. More than 200 individual pollen tubes were selected for length measurement. Values represent mean ± SE. The statistical analysis was performed by one-way ANOVA followed by a Least Significant Difference post hoc multiple comparison; capital letters indicate differences at $P < 0.01$.

(**L**) Pollen tube width was significantly increased in *vln2 vln5* plants. Plants of

different genotypes were incubated for 2 h (WT, *vln2*, *vln5*) or 4 h (*vln2 vln5*) in germination medium. More than 50 individual pollen tubes were selected for width measurement. Values represent mean ± SD. The statistical analysis was performed by one-way ANOVA followed by a Least Significant Difference post hoc multiple comparison; capital letters indicate differences at $P < 0.01$.

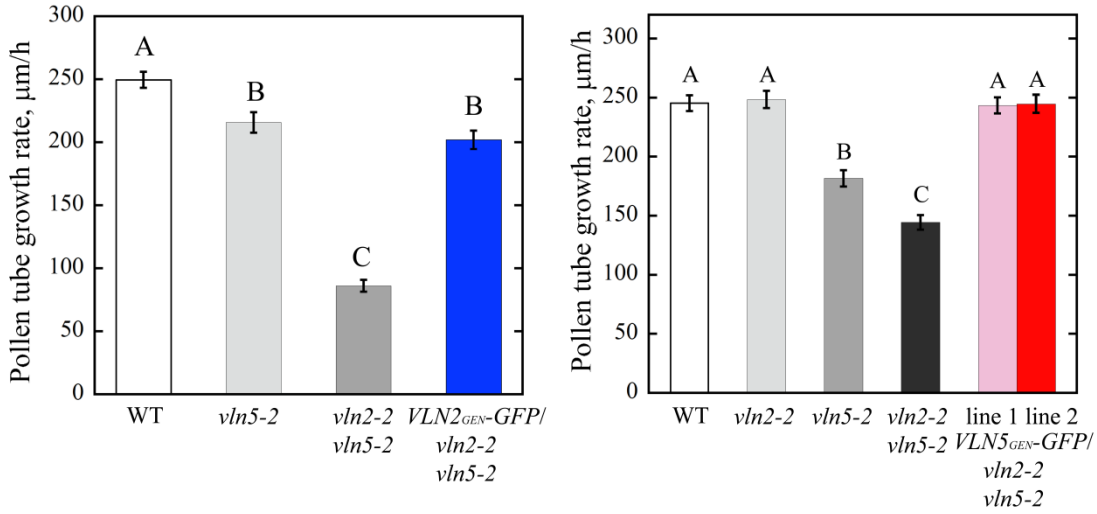

Supplemental Figure 2. VLN2$_{GEN}$-GFP and VLN5$_{GEN}$-GFP are Functional

(A) VLN2$_{GEN}$-GFP is functional in *vln2 vln5* pollen tubes. Transformation of a plasmid carrying *VLN2$_{GEN}$-GFP* into *vln2-2 vln5-2* restores the extent of pollen tube growth to a length similar to that of *vln5*, suggesting that VLN2$_{GEN}$-GFP rescues the defect caused by loss of *VLN2*. The statistical analysis was performed by one-way ANOVA followed by a Least Significant Difference post hoc multiple comparison; capital letters indicate differences at $P < 0.01$.

(B) VLN5$_{GEN}$-GFP is functional in *vln2 vln5* pollen tubes. Transformation of a plasmid carrying *VLN5$_{GEN}$-GFP* into *vln2-2 vln5-2* restores pollen tube growth to a similar extent as in the WT, suggesting that VLN5$_{GEN}$-GFP rescues the defect caused by loss of *VLN5*. The statistical analysis was performed by one-way ANOVA followed by a Least Significant Difference post hoc multiple comparison; capital letters indicate differences at $P < 0.01$.

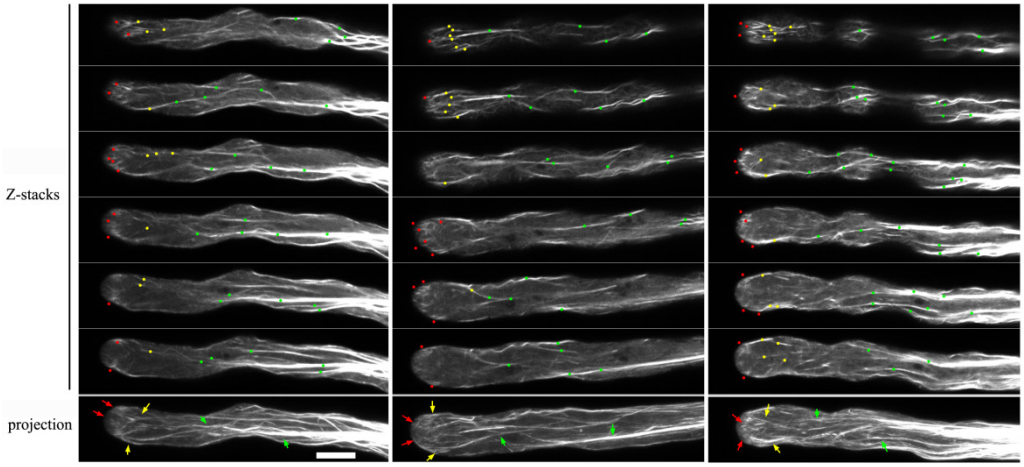

Supplemental Figure 3. Lifeact-EGFP Decorates Distinct Actin Arrays in *Arabidopsis* pollen tubes

Lifeact-EGFP decorates actin structures in the apex, subapex, and shank of *Arabidopsis* Col-0 pollen tubes. Three representative pollen tubes are presented, and the images show optical sections from z-stacks and projections. Red dots and red arrows indicate actin filaments in the apical regions of pollen tubes, yellow dots and yellow arrows indicate actin filaments in the subapex, and green dots and green arrows indicate actin cables in the shank region. Scale bar = 5 μm.

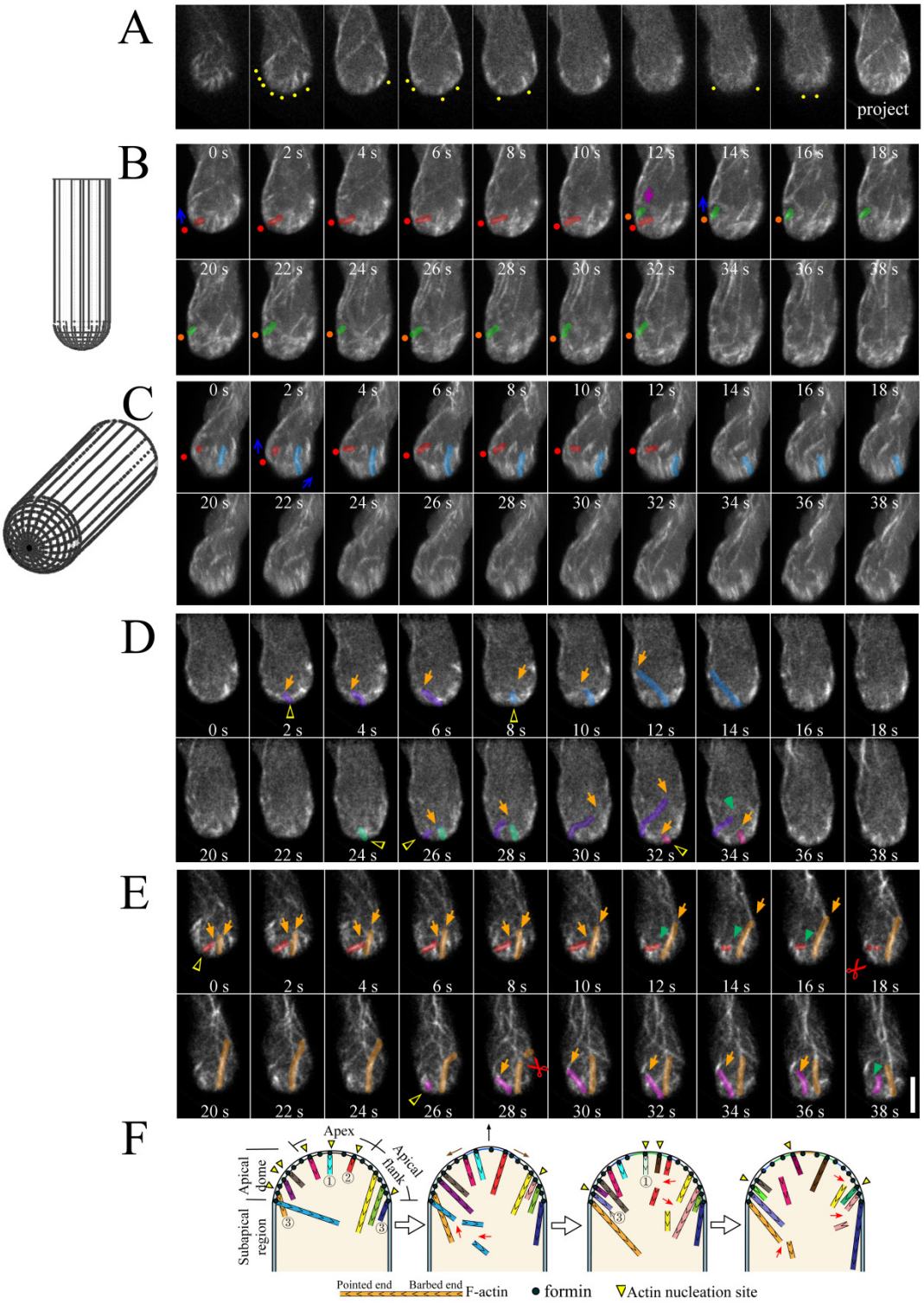
A
project
B
0 s
2 s
4 s
6 s
8 s
10 s
12 s
14 s
16 s
18 s
20 s
22 s
24 s
26 s
28 s
30 s
32 s
34 s
36 s
38 s
C
D
E
F
Apex
Apical dome
Apical flank
Subapical region
Pointed end
Barbed end
F-actin
formin
Actin nucleation site

Supplemental Figure 4. Actin Filaments are Less Abundant at the Apex and Are Highly Dynamic within the Apical Dome of WT Pollen Tubes

(**A**) Actin filaments are present at the apex and the apical flank within the apical dome. Yellow dots indicate the sites at which actin filaments are near the membrane.

(**B**) Actin filaments are constantly generated from the apical membrane and are highly dynamic. Images show projections of optical sections. Growing actin filaments were pseudocolored with different colors. Red dots and orange dots indicate the sites at which actin filaments are associated with the plasma membrane. Blue arrows indicate the direction of movement of actin filaments in transit from the apex to the apical flank. The purple arrow indicates a site at which an actin filament is nucleated at the membrane of the apical flank. See Supplemental Movie 1 online for the entire series.

(**C**) The time-lapse projection of images shown in (**B**) were rotated 45° to better visualize the apex. Red and blue pseudocolored actin filaments move from the apex to the apical flank. Blue arrows indicate the direction of movement of actin filaments in transit from the apex to the apical flank. See Supplemental Movie 2 online for the entire series.

(**D**) Actin filament dynamics in the medial optical section. Actin filaments were pseudocolored with different colors, and yellow triangles indicate the position of their nucleation. Growing and shrinking actin filaments are indicated by orange and green arrows, respectively. See Supplemental Movie 3 online for the entire series.

(**E**) Actin filament dynamics in the cortical region within the apical dome. Three actin filaments were pseudocolored red, orange, and pink. Growing and shrinking actin filaments are indicated with orange and green arrows, respectively. Scissors indicate filament severing events. Scale bar = 5 μm for images in (**A**), (**B**), (**C**), (**D**) and (**E**). See Supplemental Movie 4 online for the entire series.

(F) Schematic diagram showing actin filament dynamics within the apical dome. Actin filaments are nucleated at the apical membrane, a process likely mediated by membrane-anchored formin(s) (Cheung et al., 2010). The membrane-originated actin filaments are highly dynamic, growing and shrinking rapidly, and undergoing frequent severing events. Apex-originated and -associated actin filaments can move to the

apical flank, most likely due to the fusion of exocytic vesicles at the tip. Actin filament severing facilitates departure of actin filaments from the membrane. ① marks actin filaments that nucleated from the membrane at the apex, ② marks actin filaments moved from the apex to the apical flank and ③ marks actin filaments that nucleated from the membrane at the apical flank. Red arrows indicate severing events. Black arrow indicates pollen tube growth direction, brown arrows indicate the direction of membrane flow.

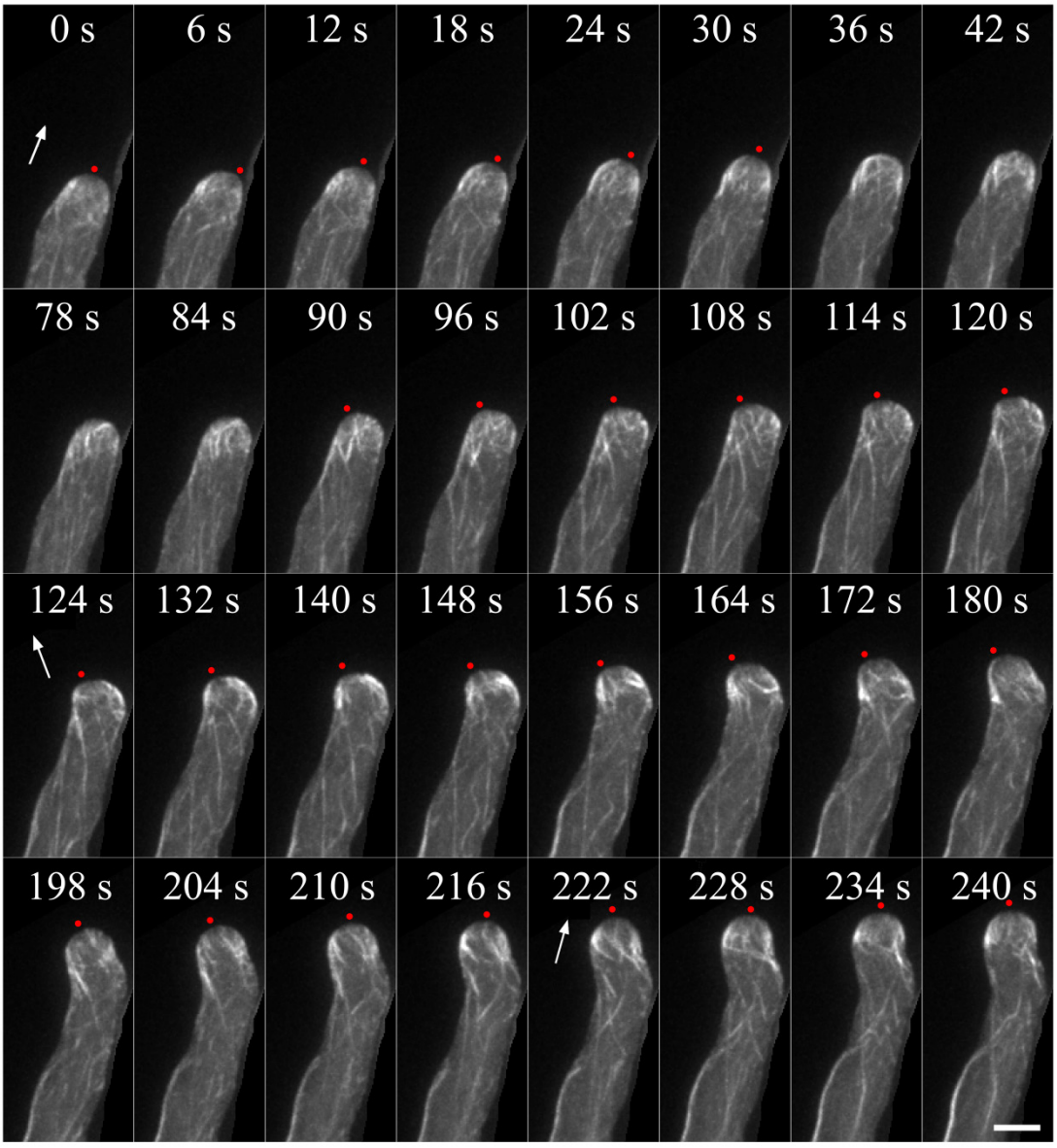

Supplemental Figure 5. The Extreme Apex Has Fewer Actin Filaments and Faces the Direction of Growth

Time-lapse series showing actin filaments during pollen tube growth. Red dots mark the extreme apex of the growing pollen tube, which faces the direction of growth. White arrows indicate the direction of growth. Scale bar = 5 μm.

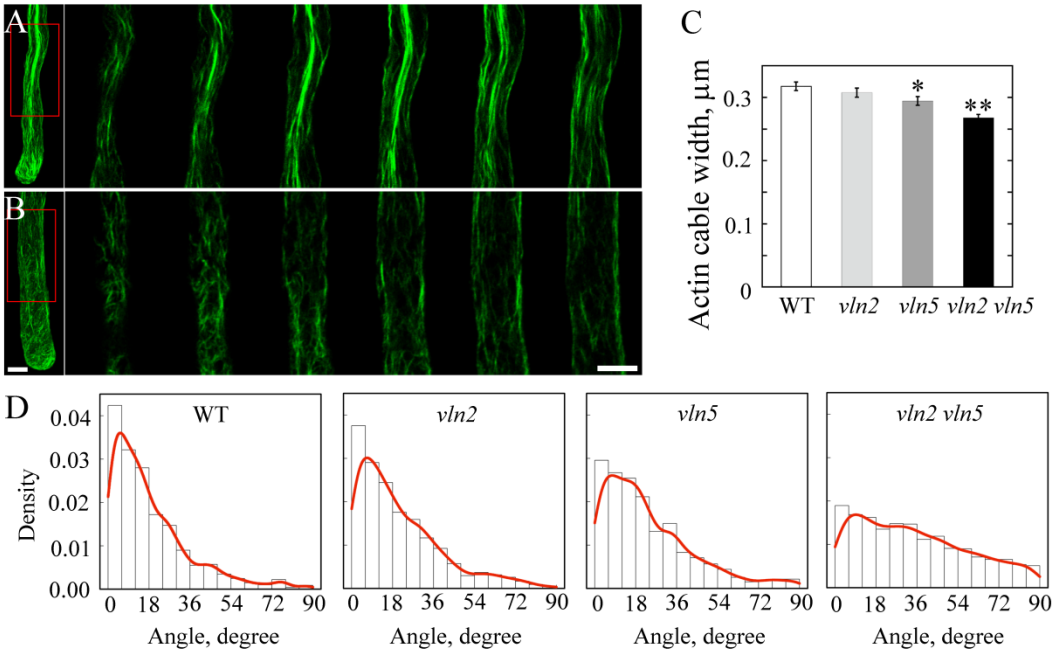

Supplemental Figure 6. The width of Actin Cables Was Decreased and Angles Formed Between Actin Cables and The Growth Axis of Pollen Tubes Increased in *vln2 vln5* Pollen Tubes

(A) and **(B)** Visualization of actin filaments in the shank region of WT **(A)** and *vln2 vln5* **(B)** pollen tubes. The projection (left panel) and selected optical sections are shown. The red box marks the shank region containing the longitudinal actin cables. Scale bars = 5 μm.

(C) The width of actin cables was decreased in the shank of *vln5* and *vln2 vln5* pollen tubes. At least 120 cables from 5 pollen tubes were selected for analysis. Values represent mean ± SE, *P < 0.05 and **P < 0.01 by a Student's *t*-test.

(**D**) The angles formed between actin cables and the growth axis of pollen tubes increased in *vln5* and *vln2 vln5* pollen tubes. The histograms of angles for WT, *vln2*, *vln5* and *vln2 vln5* pollen tubes are present. Red lines are the kernel density estimation of the distribution of the angles. At least 900 actin cables from 10 individual pollen tubes were selected for the measurement.

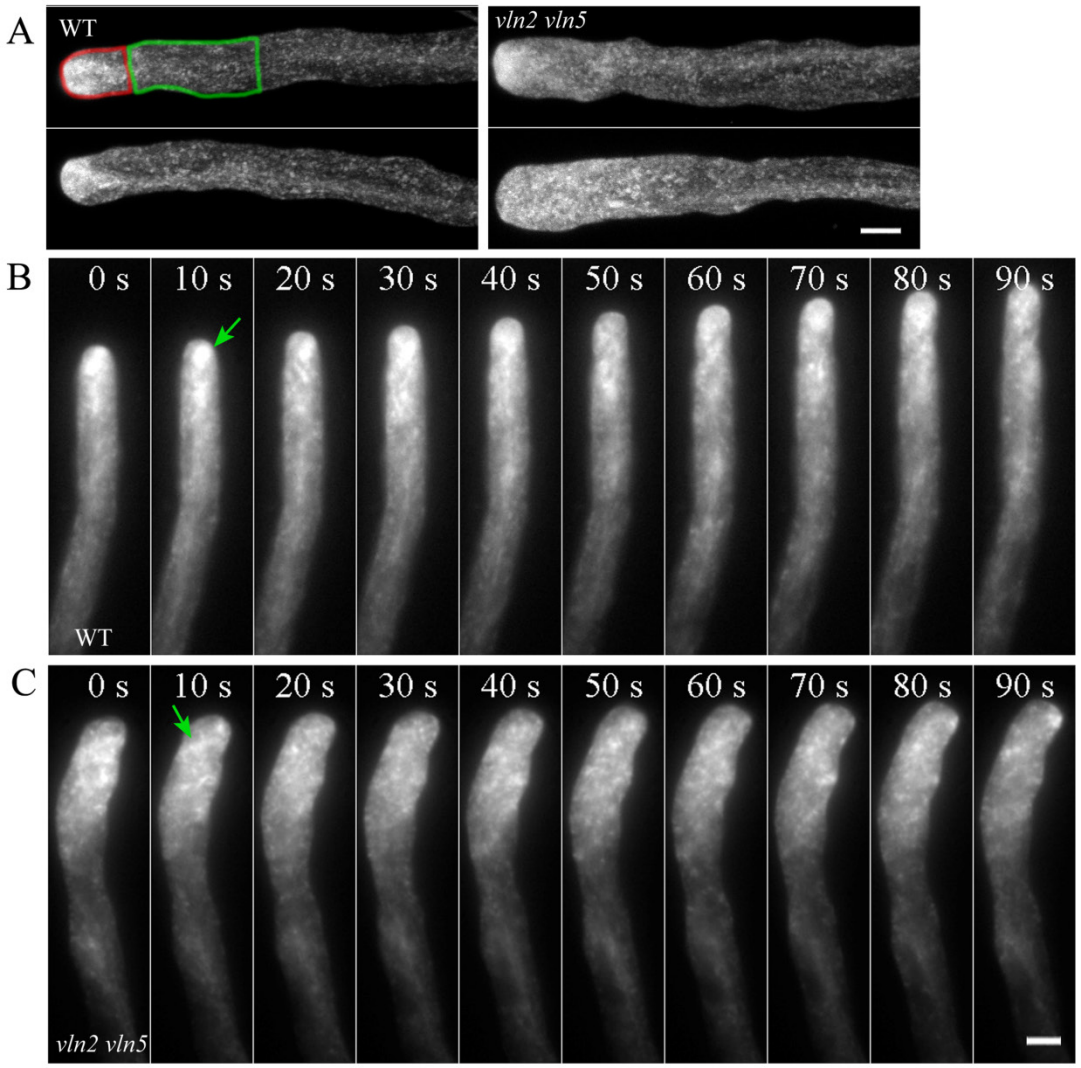
A
WT
vln2 vln5
B
0 s
10 s
20 s
30 s
40 s
50 s
60 s
70 s
80 s
90 s
WT
C
0 s
10 s
20 s
30 s
40 s
50 s
60 s
70 s
80 s
90 s
vln2 vln5

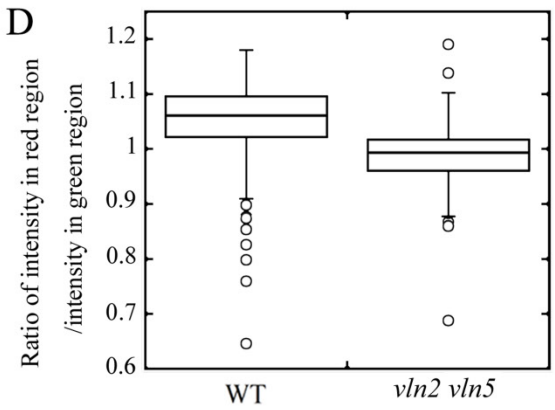
D
Ratio of intensity in red region
/intensity in green region
1.2
1.1
1
0.9
0.8
0.7
0.6
WT
vln2 vln5

Supplemental Figure 7. The Distribution of Rab4Ab-labeled Vesicles Is altered in *vln2 vln5* Pollen Tubes

(**A**) Projections of pollen tubes expressing YFP-RabA4b. The left and right panels show WT and *vln2 vln5* pollen tubes, respectively. Fluorescence levels in the red box were divided by fluorescence levels in the green box to yield a ratio reflective of the distribution of vesicles in (**D**). Scale bar = 5 μm.

(**B**) Time-lapse images of a WT pollen tube expressing Lat52:YFP-RabA4b. Green arrow indicates the concentrated location of YFP-RabA4b-labeled vesicles. See Supplemental Movie 14 online for the entire series.

(**C**) Time-lapse images of a *vln2 vln5* pollen tube expressing Lat52:YFP-RabA4b. Green arrow indicates the concentrated location of YFP-RabA4b-labeled vesicles. See Supplemental Movie 15 online for the entire series. Scale bar = 5 μm for images in (**B**) and (**C**).

(**D**) Quantification of the distribution of YFP-RabA4b-labeled vesicles in WT and *vln2 vln5* pollen tubes. The ratio was defined in (**A**). The ratio decreased in *vln2 vln5* pollen tubes.

REFERENCES

Cheung, A.Y., Niroomand, S., Zou, Y.J., and Wu, H.M. (2010). A transmembrane formin nucleates subapical actin assembly and controls tip-focused growth in pollen tubes. Proc. Natl. Acad. Sci. USA **107,** 16390-16395.

Supplemental Table 1. Primer sequences used in this study

Primer name	Primer sequence
V2F1	5'-GCCCATGGCAACAAAAGTGTTGGATCCT-3'
V2R1	5'-GCGCGGCCGCCTAGAACAAGTCGAACTTCTT-3'
V5F1	5'-GCCCATGGCGTTTTCCATGAGAGATTTA-3'
V5R1	5'-CGGCGGCCGCTTAGAAGAGATTGACAGACAT-3'
$V2_{GEN}F$	5'-GGGGACAAGTTTGTACAAAAAAGCAGGCTTCTTCAGGAATGGCTCTTTTG-3'
$V2_{GEN}R$	5'-GGGGACCACTTTGTACAAGAAAGCTGGGTCGAACAAGTCGAACTTCTTCT-3'
$V5_{GEN}F$	5'-GGGGACAAGTTTGTACAAAAAAGCAGGCTACTCGTTAGTCCGTTTTGTT-3'
$V5_{GEN}R$	5'-GGGGACCACTTTGTACAAGAAAGCTGGGTCGAAGAGATTGACAGACATTT-3'
eIF4AF	5'-GGGTATCTATGCTTACGGTTTCG-3'
eIF4AR	5'-CAGAGAACACTCCAACCTGAATC-3'